Quasi Two-Dimensional Dye-sensitized In_2O_3 Phototransistors for Ultra-High Responsivity and Photosensitivity Photodetector Applications

Alexander D Mottram[1], Yen-Hung Lin[1], Pichaya Pattanasattayavong[1,2], Kui Zhao[3], Aram Amassian[3], & Thomas D. Anthopoulos[,1]*

AUTHOR ADDRESS

[1]Centre for Plastic Electronics and Department of Physics, Blackett Laboratory, Imperial College London, London, SW7 2BW, United Kingdom

[2]Department of Materials Science and Engineering, School of Molecular Science and Engineering, Vidyasirimedhi Institute of Science and Technology, Wangchan, Rayong, 21210, Thailand

[3]Materials Science and Engineering, Division of Physical Sciences and Engineering, Solar and Photovoltaics Engineering Research Center (SPERC), King Abdullah University of Science and Technology, Thuwal 23955-6900, Saudi Arabia

KEYWORDS: Metal oxide transistor, photodetector, phototransistor, responsivity, photosensitivity, indium oxide

ABSTRACT

We report the development of dye-sensitized thin-film phototransistors consisting of an ultra-thin layer (<10 nm) of indium oxide (In_2O_3) the surface of which is functionalized with a self-assembled monolayer of the light absorbing organic dye D102. The resulting transistors exhibit a preferential color photoresponse centered in the wavelength region of ~500 nm with a maximum photosensitivity of $\sim 10^6$ and a responsivity value of up to 2×10^3 A/W. The high photoresponse is attributed to internal signal gain and more precisely to charge carriers generated upon photoexcitation of the D102 dye which lead to the generation of free electrons in the semiconducting layer and to the high photoresponse measured. Due to the small amount of absorption of visible photons the hybrid In_2O_3/D102 bilayer channel appears transparent with an average optical transmission of >92 % in the wavelength range 400-700 nm. Importantly, the phototransistors are processed from solution-phase at temperatures below 200 °C hence making the technology compatible with inexpensive and temperature sensitive flexible substrate materials such as plastic.

1. Introduction

Research into photodetectors has been intensified by the desire to produce more complex and multifunctional electronic components such as touch screens with integrated photodetectors,[1] stacked color pixel sensors,[2] and photosensitive screens.[3] High responsivity, high photosensitivity, low noise, and stable performance have always been key factors in the assessment of a good photodetector, but now extra demands are being made of these devices.

These new requirements include color selectivity, transparency, scalable low-cost manufacturing, low-temperature processes, and integrated gain mechanisms.

One device structure with the potential to fulfill many of these requirements comes from the combination of the two well established fields of thin-film transistors[4] (TFTs) and dye-sensitized solar cells[5] (DSSCs). DSSCs use small organic molecules or metallic complexes with bonding groups chosen for semiconductor compatibility as the light harvesting component in a solar cell. While the gate-induced field effect of a transistor can be used to modify the optoelectronic response of the semiconducting film being operated as a lateral photoconductor.[6] It has been demonstrated separately that transistors based on SnO_2 nanowires and ZnO thin films can be functionalized with chlorophyll, fluorescein and D102 to produce photosensitive transistors.[7,8] The D102-dyed ZnO transistors produced by the latter exhibited a high responsivity of 1×10^4 A/W and a photosensitivity of 1×10^6, comparable to state-of-the-art devices (**Figure 1**) but required processing temperatures of 400°C.[8]

Here we report on low temperature (≤ 200 °C) solution-processed, dye-sensitized thin-film transistors (DSTFTs) based on In_2O_3 as the semiconducting channel. A unique characteristic of these devices is the ultra-thin nature of the In_2O_3 layers (~7 nm-thick), which enables functionalization of the D102 dye in close proximity to the active device channel. This unique dimensionality offers improved electronic coupling between the transistor channel and the light-absorbing dye. Effective functionalization of the latter onto the In_2O_3 layers is verified by optical absorption measurements which reveal the existence of an additional absorption peak at ~500 nm superimposed on the absorption spectra of the In_2O_3 layer. Different color light-emitting diodes (LEDs) were used to photoexcite the hybrid photoactive layers during which the operating characteristics of the transistors were monitored. From these measurements we show that dye-

sensitization increases the device photosensitivity and responsivity to all incident wavelengths, with the biggest effect observed under green light illumination. Best performing phototransistors exhibit a maximum responsivity of ~2×10^3 A/W and a photosensitivity of 1×10^6. Due to its ultra-thin nature, the photoactive In_2O_3/D102 layer is extremely transparent with a minimum transmission of 92 % across all visible wavelengths (400-700 nm). The successful demonstration of dye-sensitized In_2O_3 phototransistors can be seen as a step towards transparent and highly sensitive photodetectors processed from solution at low temperature.

2. Experimental Techniques

2.1. Device Fabrication

Highly doped p-type silicon (Si^{++}) wafers with a 400 nm-thick thermally grown silicon dioxide (SiO_2) layer were used to fabricate bottom-gate, top source-drain (S-D), thin-film transistors. The Si^{++}/SiO_2 substrates were cleaned in deionized water, acetone, and IPA in an ultrasonic bath for approximately 10 min each. UV/ozone exposure was then carried out in order to remove any organic residues and improve the wettability for solution-phase deposition. Anhydrous indium nitrate [$In(NO_3)$] was dissolved in deionized water at a concentration of 40 mg/mL. The solution was then stirred at room temperature for 1 h before use. The indium oxide (In_2O_3) layer was deposited onto the substrates using spin casting at 4000 rpm for 30 s, followed by a 2 h thermal annealing at 200 °C. For dye functionalization, the freshly-prepared In_2O_3 films were sensitized with the light-absorbing organic molecule D102 by immersing the sample into a 0.8-mM solution of D102 with a 50:50 vol.% mix of acetonitrile and tert-butanol for 1 min. Excess dye was washed off with deionized water and the samples were dried with nitrogen. Pristine control

samples were left untreated during the process of dye functionalization for comparative measurements. Transistor fabrication was finished with the thermal evaporation of aluminum source/drain (S/D) contacts under high vacuum (10^{-6} mbar) using shadow masks.

2.2 Material Characterization

The surface morphologies of the functionalized and control samples were studied using an atomic force microscope (Agilent 5500 AFM) in intermittent contact mode. Film transmittance was measured using a Shimadzu 2600 UV-Vis spectrophotometer. The samples for UV-Vis measurement were produced on cleaned quartz in an identical method as on Si^{++}/SiO_2. High-resolution transmission electron microscopy (HR-TEM) images were performed on control In_2O_3 films on Si^{++}/SiO_2 substrates using a Titan 80-300 Super Twin microscope operating at 300 kV.

2.3 Optoelectronic Characterization

Optoelectronic characterization was performed in a nitrogen atmosphere by measuring the transfer characteristics of fabricated transistors at a fixed source-drain voltage (V_D) of 5 V under various levels of irradiance from three LEDs. The LEDs colors and their peak wavelengths' were red (λ_{peak} = 630 nm), green (λ_{peak} = 522 nm), and blue (λ_{peak} = 470 nm). The LED current was controlled with a Keithley 2400 source meter and the power intensity was measured using a Gentec-eo XLP12-3S-H2 calibrated thermopile in close proximity to the transistors. Electrical properties of the transistors were measured using an Agilent B2902A source/measure unit at room temperature. Although the rise time (switch-on time) of the channel current for all phototransistors upon illumination is found to be < 1 s, all devices were illuminated for a 30 s

before the transfer characteristics were acquired using a scan rates of 1 V/s. For each measurement additional scans were performed in order to ensure that the measured device response was stable under different illumination intensities and parasitic effects such as bias-stress were not prominent. The channel width and length of all transistors investigated were 1 mm and 50 μm, respectively. The geometric capacitance of the SiO_2 dielectric employed was 8.6 nF/cm^2.

Two figures of merit have been used to assess the response of each transistor as a photodetector, the responsivity (R) and photosensitivity +(PS). The responsivity, also known as the photoresponsivity, is defined as the change in current ($\Delta I = I_{illum} - I_{dark}$) per unit of incident illumination power (P_{illum}) and is given by:

$$R = \frac{I_{illum} - I_{dark}}{P_{illum}} \ [\mathrm{A/W}] \qquad (1)$$

Here, I_{illum} and I_{dark} are the drain current of the transistor under illumination and in the dark, respectively. Responsivity is a function of applied gate voltage (V_G) and is normalized to the incident light power as opposed to the incident light intensity such that photodetectors with small active areas exhibit greater responsivity even though the change in current is significantly smaller. As such, small-area, low-dimensional flake-based devices dominate the high responsivity region of **Figure 1**. However, the relative change in current with respect to the dark current is also crucial to an instrumented photodetector.[28,29] The photosensitivity (PS) is the change in current (ΔI) normalized to the dark current:

$$PS = \frac{I_{illum} - I_{dark}}{I_{dark}} \qquad (2)$$

Here, the PS is also a function of the applied gate voltage (V_G) and the illumination power implicitly through the channel current response. Although the PS is not normalized for incident

power, and hence hard to compare for different illumination intensities, it does provide valuable information of how a device will function as a photodetector.

2.4 Bandgap Density of States (DOS) Analysis

The density of states (DOS) in the bandgap can be used to measure the shift of the Fermi level towards the conduction band upon illumination. To extract the DOS and study the strength of the photodoping, a method developed originally by Grünewald et al.,[30] was adopted. Its advantage over most other methods of DOS extraction is that it does not require temperature dependent measurements while producing comparable results to other methods.[31] The DOS analysis relies on two main assumptions: firstly that transport through the material is limited by multiple trapping and thermal release,[32,33] and secondly that there is a conduction band edge, above which the conduction band DOS is assumed to be constant with fixed electron mobility and below which exists only traps that produce a localized bandgap DOS. These bandgap states control the subthreshold characteristics of a TFT and the measured field effect mobility via the relative fraction of charge carriers distributed in immobile and mobile states. As the gate voltage of a TFT is increased charge is accumulated into the channel. Through analysis of the rate of increase in conductance with accumulated charge, it is possible to work backwards and calculate the form of the bandgap DOS. The electric potential through the semiconductor can be analytically calculated from simple electrostatics using a thick film approximation.[34] From this a relationship between the surface potential at the insulator-semiconductor interface (V_0) and the accumulated charge at the surface [$n(V_0)$] can be derived using:

$$n(V_0) = -\frac{C_i^2}{q\epsilon_s\epsilon_0} V_F \left(\frac{dV_0}{dV_F}\right)^{-1} \qquad (3)$$

where, C_i is the geometric capacitance of the TFT, q is the elementary charge, ϵ_s and ϵ_0 are the relative permittivity of the semiconductor and the permittivity of free space, respectively. V_F is the applied voltage defined as $V_F = V_G - V_{FB}$, where V_{FB} is the flat-band voltage, commonly assumed to be equal to the turn-on voltage. The relation between surface potential and applied voltage is:

$$\exp\left(\frac{qV_0}{k_BT}\right) - \frac{qV_0}{k_BT} - 1 = \frac{qC_i d_s}{k_BT\epsilon_s\epsilon_0 I_0}\left[I_D(V_F)V_F - \int I_d(V_F)dV_F\right] \qquad (4)$$

where k_B is the Boltzmann constant, T is the measurement temperature, d_s is the thickness of the semiconducting layer, $I_D(V_F)$ is the measured current at applied voltage V_F and I_0 is the current when $V_F = 0$. **Equation (4)** must be solved for each measured gate voltage point to create a set of matched points of V_0 and V_F which, when inserted into **Equation (3)**, will give a series set of points of $n(V_0)$ against V_0. The accumulated charge is related to the DOS of the material via a convolution of the DOS with the Fermi-Dirac distribution $[f(E)]$, minus the charge present at flat-band, as follows:

$$n(V_0) = \int g(E)[f(E - V_0) - f(E)]dE \qquad (5)$$

where E is the energy above the Fermi level and $g(E)$ is the semiconductor DOS. Deconvolution of **Equation (5)** can be approximated as a differential using a low temperature approximation:[31]

$$g(E) \approx \frac{1}{q}\frac{d}{dV_0}[n(V_0)] \qquad (6)$$

yielding the bandgap DOS as a function of energy above the Fermi level at flat-band voltage.

3 Results and Discussion

3.1. Film Characterization and Functionalization

Figure 2a shows the lower and higher magnification cross-sectional HR-TEM images of a representative In_2O_3 layer deposited by spin-coating on SiO_2. The resulting layers are ultrathin and highly polycrystalline with an average film thickness of ~7 nm. It has recently been shown that such thin In_2O_3 layers exhibit significant energy quantization effects owing to the carrier confinement in the out-of-plane direction.[35–38] Most importantly, devices based on such thin layers are likely to exhibit extreme sensitivity to electrostatic changes taking place at the surface of In_2O_3 layers due to its proximity to the active channel forming at the dielectric/semiconductor interface. It is therefore reasonable to assume that when the D102 dye binds to the surface of the In_2O_3 layer via its carboxylic anchoring group,[39,40] any change in the excited state of the dye will be strongly coupled to the active channel of the transistor.

The presence of D102 on the surface of the In_2O_3 layer was confirmed using UV-Vis spectroscopy (**Figure 2b)**, which reveals the appearance of an additional absorption peak. In particular, In_2O_3/D102 bilayers show a wide absorbance peak centered at ~500 nm, corresponding to the absorption peak of the D102 dye,[41] as well as an increase in absorbance across all wavelengths when compared to the control In_2O_3 layer. The latter shows a small amount of absorbance that increases <400 nm as expected due to interband absorption. Importantly, the total transmittance of the dye-functionalized In_2O_3 layer is found to be very high and >92% across the visible wavelengths making these hybrid In_2O_3/D102 bilayers extremely transparent. We assume a complete coverage of the In_2O_3 films with D102 as it was visually observed on In_2O_3 layers grown on quartz substrates. Dye coverage on In_2O_3 films grown on Si^{++}/SiO_2 wafers was impossible to evaluate due to the reflective nature of the wafer. On the basis of this measurement and the AFM analysis, which will be discussed later (**Figure 3**), we propose that the D102 forms a complete monolayer on the surface of the ultra-thin In_2O_3. Further

evidence supporting this assumption comes from the independence of the absorption of In_2O_3/D102 bilayer on the immersion time used to functionalize the D102 on In_2O_3.

The impact of dye-functionalization on the In_2O_3 surface topography was studied by AFM in an effort to identify any possible conglomeration of the D102 dye. The AFM topography images (0.5 μm × 0.5 μm) of the control In_2O_3 and the In_2O_3/D102 bilayer samples are shown in **Figure 3a.** Both samples exhibit nearly identical surface features with comparable surface roughness root-mean-square (rms) values of ~0.2 nm. Quantifiable confirmation of the similarity between control and D102-functionalized In_2O_3 channels are shown in the height distribution histograms in **Figure 3b** where no difference between the two samples can be identified. On the basis of these observations, it is suggested that D102 forms a molecularly-thin monolayer on the surface of the In_2O_3 without any apparent conglomeration.

3.2. Optoelectronic Characterization of In_2O_3/D102 Bilayers

The impact of dye-functionalization on the charge transport properties of In_2O_3 layers has been investigated using field-effect measurements. **Figures 4a** and **4b** show the schematics of the control and D102-sensitized transistors architectures used. Since variation in the operating characteristics of metal oxide transistors such as turn-on voltages (V_{on}) and threshold voltages (V_{Th}) is commonly reported in the literature,[42,43] and often attributed to ambient conditions,[44] electrical measurements of both devices were undertaken under inert atmosphere. Furthermore, we verified that functionalization of D102 onto the In_2O_3 channels does not cause any major change in the transistor's operating characteristics, nor is there any major difference between the dark transfer characteristics measured for the D102-sensitized and control devices.

Figures 4c-h display the transfer characteristics for both the control and D102-sensitized transistors measured in the dark and under optical illumination using three different color inorganic LEDs (**Figure 4i**). Control devices characterized in darkness exhibit electron mobilities of ~1 cm^2/Vs and show no response to red light (**Figures 4c**), a small response to green light (**Figures 4e**) and a large response to blue light (**Figures 4g**). These observations correlate with the product of the overlap of absorbance of the control film with the electroluminescent (EL) spectra of the LEDs used (**Figure 4i**). The observed transistor photoresponse consists of two key components: (i) a shift in the V_{on} voltage toward negative gate voltages (V_G), and (ii) an increase in the transistor's channel off-current (I_{off}). There exists a small difference in I_{off} between the two lowest illumination intensities for the control device under blue light illumination in **Figure 4g**. We attribute this to a change in the integration time used during electrical characterization of the devices. In all other cases the lowest value of I_{off} was set by the sensitivity of the semiconductor parameter analyzer used (~10^{-11}A).

The dye-sensitized transistor responds moderately to red light illumination but shows very large responses to both green and blue photons. Again the response consists of both a negative shift in V_{on} and a significantly more obvious increase in I_{off}. Once more, the magnitude of the photoresponse correlates with the overlap of the emission spectra of the LEDs and the absorption spectrum of the D102-sensitized In_2O_3 layer.

Three mechanisms are likely responsible for causing the change in the transistor transfer characteristics. The first proposed mechanism is photoconduction, where excitation of electrons and holes from impurity states due to absorbed photons increase the channel's off-current. Considering first the In_2O_3 film, states within the bandgap allow for photons to be absorbed below the bandgap energy creating transient charge carriers that produce a measurable

photocurrent.[45] A common approximation within amorphous and polycrystalline materials is that the bandgap density of states (DOS) exponentially decays with energy away from the conduction band,[46,47] leading to greater photocurrent for shorter wavelengths. The photocurrent is several orders of magnitude lower than any induced field-effect current, and hence will only be observable in the off-state of the transistor. For the control device, the increase in the off-current is clearly visible under blue light illumination (**Figure 4g**) but is too small to be apparent (compared to the experimental noise floor) under green (**Figure 4e**) and red (**Figure 4c**) light. Based on these findings we conclude that the observed In_2O_3 I_{off} photoresponse to blue photons is most likely attributed to photoconduction, but this does not provide a good explanation for the negative shift in V_{on}.

The second mechanism is photon absorption by the D102 layer followed by electron transfer from the lowest occupied molecular orbital (LUMO) of D102 (-2.59 eV) to the conduction band (CB) of In_2O_3 (-3.98 eV eV).[35,48,49] Based on the materials energetic, the latter process is indeed favorable and is expected to increase the electron concentration within the device's ultra-thin channel. This process is expected to shift the V_{on} towards more negative gate voltages and/or increase the off-current of the transistor, in qualitative agreement with the data shown in **Figures 4f** and **4h**, where D102-sensitized transistors exhibit an enhanced off-currents when measured under green and blue light illumination. The level of increase in these two cases is similar, which is expected as the overlap between the absorbance spectrum of the In_2O_3/D102 layer and the EL spectra of the green and blue LEDs is of the same order. Thus transfer of photogenerated electrons from D102 to In_2O_3 explains the increase in the off-current seen in the dye-functionalized In_2O_3 transistors as compared to the control devices based on pristine In_2O_3, but not the negative shift in V_{on}.

The third possible process that could also explain the observed shift in V_{on} is photodoping, which results from desorption of molecular oxygen from the surface of In_2O_3 upon illumination. This process has been proposed by *Verbakel et al*. to explain the increase in conductivity in ZnO nanoparticle based diodes and TFTs,[50] while *Lakhwani et al*. argued that the same process is responsible for the creation of a Moss-Burstein shift in ZnO nanoparticles-composed films upon UV illumination.[51] In the proposed process, surface bound oxygen molecules act as electron traps which tend to deplete the semiconductor of mobile electrons. Introduction of holes, most likely via photogeneration due to interband absorption [injection of holes directly to the valence band (VB) of In_2O_3 (-7.85 eV)[35] from the Al S-D electrodes is highly unlikely due to the large potential barrier], results in desorption of oxygen and to an increase in the electron concentration within the channel. In a nitrogen atmosphere oxygen desorption is likely to be manifested as a relatively long-term effect since there are only a few molecules to be reabsorbed. *Kim et al*.[52] has argued that oxygen desorption will lead to the creation of a back channel which can in turn increase the overall conduction of the device. The low dimensional nature of the In_2O_3 layers used here makes it very likely that the oxygen depleted surface is an integral part of the channel and effectively acts as an efficient form of photodoping. However, further work is needed in order to prove or refute the proposed mechanisms.

3.3. Gate-Field Dependent Photoresponse

The photosensitivity and the responsivity are important figures of merit that are associated with diodes and photoconductors, so a TFT operated as a phototransistor is best considered as a photoconductor, the channel conductivity of which can also be modified by the applied gate-field. The photosensitivity and responsivity will therefore depend on gate voltage and so should

be calculated as a function of V_G to find the optimum operating regime. The photosensitivity and responsivity of the In_2O_3/D102 based transistors to green light as a function of V_G is shown in **Figure 5**. Here, green illumination was chosen since it showed the biggest difference in response between dye-sensitized and control devices.

The photosensitivity of the functionalized device to green light peaks at $V_G = 10$ V (**Figure 5a**) with a maximum value of $>10^5$. This is expected as it is the point where the device is about to be turned-on so the photodoping shifts the transistor into the subthreshold operating regime. The responsivity of the device, on the other hand, increases with increasing V_G and at -10 V illumination with lower intensities produce a greater change in current per watt (A/W) of incident optical power than higher irradiance levels (**Figure 5b**). We attribute this to the response being cumulative over time till it reaches equilibrium, such that increasing illumination intensity produces diminishing gains as there will be less oxygen available to desorb, hence a smaller photodoping effect.

3.4. Wavelength Dependent Photoresponse

To compare the photoresponse of the control and D102-sensitized phototransistors to different color LEDs, a V_G potential was selected using **Figure 5** as a guide. For the purpose of this experiment a V_G = 0 V was chosen. **Figure 6** shows the measured photosensitivity (top row) and responsivity (bottom row) for the control and dye-sensitized transistors under blue, green and red color illumination at different irradiance levels. The observable trend in **Figure 6** is that sensitization of the In_2O_3 layer with D102 increases the photosensitivity and responsivity of the channel to all colors. Specifically, the photosensitivity increases with increasing incident optical power for each D102-sensitized In_2O_3 transistor because of the exponential nature of the transfer

characteristics where the photodoping effect results to exponentially increasing currents. In other words the device exhibits high signal amplification but its response is highly non-linear to the incident optical power. On the other hand the transistor's responsivity decreases with increasing irradiance. This is not surprising since the channel current (A) remains within the same range while the incident optical power (W) increases. As a result the maximum responsivity of the device (A/W) decreases with increasing irradiance. Finally, it is worth noting that although the maximum values of photosensitivity and responsivity are measured for In_2O_3/D102 devices illuminated with blue light, the biggest change in photosensitivity is measured under green light illumination.

3.5. Photodoping and Bandgap States

Bandgap states play a very important role in TFT operation as they dominate the subthreshold slope via the trapping of charges, slowing the progress of the quasi Fermi level[53] towards the conduction band with applied V_G. From the earlier discussion it is believed that the shift of the V_{on} towards more negative gate fields is due to photo-induced n-doping of In_2O_3. The latter implies that upon illumination the Fermi energy level (E_F) of In_2O_3 shifts towards the conduction band. This section provides the analysis on the E_F shift, within the framework of a model developed by Grünewald et al.,[30] to calculate the magnitude of the photo-induced n-doping from the evolution of the calculated bandgap states due to green light illumination.

Due to the existence of a substantial number of bandgap states in oxide materials,[54,55] photodoping is very unlikely to alter the number of bandgap states without a physical change in the crystal structure of In_2O_3, such as introduction of extrinsic dopants.[56] Therefore, it is assumed there is no change in the bandgap DOS in the In_2O_3 layers. This means the only observable effect

upon irradiation should be the shift of E_F towards the conduction band. Multiple methods exist for calculating the bandgap DOS as outlined by *Kalb et al.*,[31] but the majority of those rely on extensive temperature-dependent charge transport measurements with the main assumption being that there is no temperature dependence in bandgap states.[57–59] In contrast, data analysis based on the Grünewald et al.[30] model can be performed using a single transistor transfer characteristics at any temperature. In particular, the method relies on the analysis of the subthreshold slope from which the bandgap states can be calculated. The underlying assumption is to utilize a rectangular conduction band which can be approximated to a simple differential as described by *Kalb et al.*[60] When the oxide semiconductor is photodoped, the E_F shifts towards the conduction band, and the region of the bandgap DOS being probed by the measurement will also shift accordingly. The separately calculated bandgap DOSs can then be shifted in energy for each illumination intensity, in order to line up the data with those extracted from the dark current measurements. It is then assumed that this characteristic energy shift is equivalent to the E_F displacement caused by the photo-induced n-doping of In_2O_3. Based on this simple method, the degree of photodoping can be quantified and compared to the different experimental conditions.

Several transfer characteristics obtained from D102-sensitized In_2O_3 transistors under green light illumination were used to calculate the DOS in the semiconducting channel. **Figure 7** shows the energy-adjusted DOS calculated for transistors that were electrically characterized in the dark and under green light illumination at different intensities. The inset shows the resulting E_F shift due to photo-induced doping versus green light intensity. All calculated DOS are found to be exponential in nature and well correlated upon E_F adjustment. This finding supports the hypothesis that the main mechanism for the observed shift in the transistors' operating characteristics towards negative V_G voltages, and the resulting high responsivity and

photosensitivity values, is due to photo-induced n-doping of the In_2O_3 channel. The noticeable fluctuations seen at higher energies (>0.44 eV) is attributed to the breakdown of the *Grünewald* model since the E_F approaches and even enters the conduction band of In_2O_3.

4. Conclusions

In conclusion, dye-sensitized In_2O_3 phototransistors were fabricated from solution at temperatures ≤ <200 °C. Although the resulting devices show significant photoresponse across all visible wavelengths investigated, the largest response is measured for transistors illuminated with green light due to the absorption characteristics of the D102 dye employed and the ultra-thin nature of the In_2O_3 semiconductor, clearly demonstrating the advantages of intentional channel sensitization to specific wavelengths. This simple to implement phototransistor architecture yields maximum photosensitivity of ~10^6 and a responsivity value of ~2000 A/W due to the extremely high signal gain properties of the device. The latter is attributed to the electrical gating of the photoactive channel which allows access to operating regimes that are inaccessible by conventional two-terminal photodetectors. The gating potential of the photoactive channel can in principle be reduced further either by making the gate dielectric layer thinner or through the use of high-k dielectrics such as metal oxides (e.g. HfO_2, ZrO_2, Al_2O_3). The unique attributes which include optical transparency, preferential spectral response and processing versatility make the low-dimensional In_2O_3/D102 phototransistor concept an interesting technology for the development of unusual devices such as full-color transparent photodetectors. To date only a handful of demonstrated devices satisfy these criteria making the present work poptentially interesting for future developments.

FIGURES

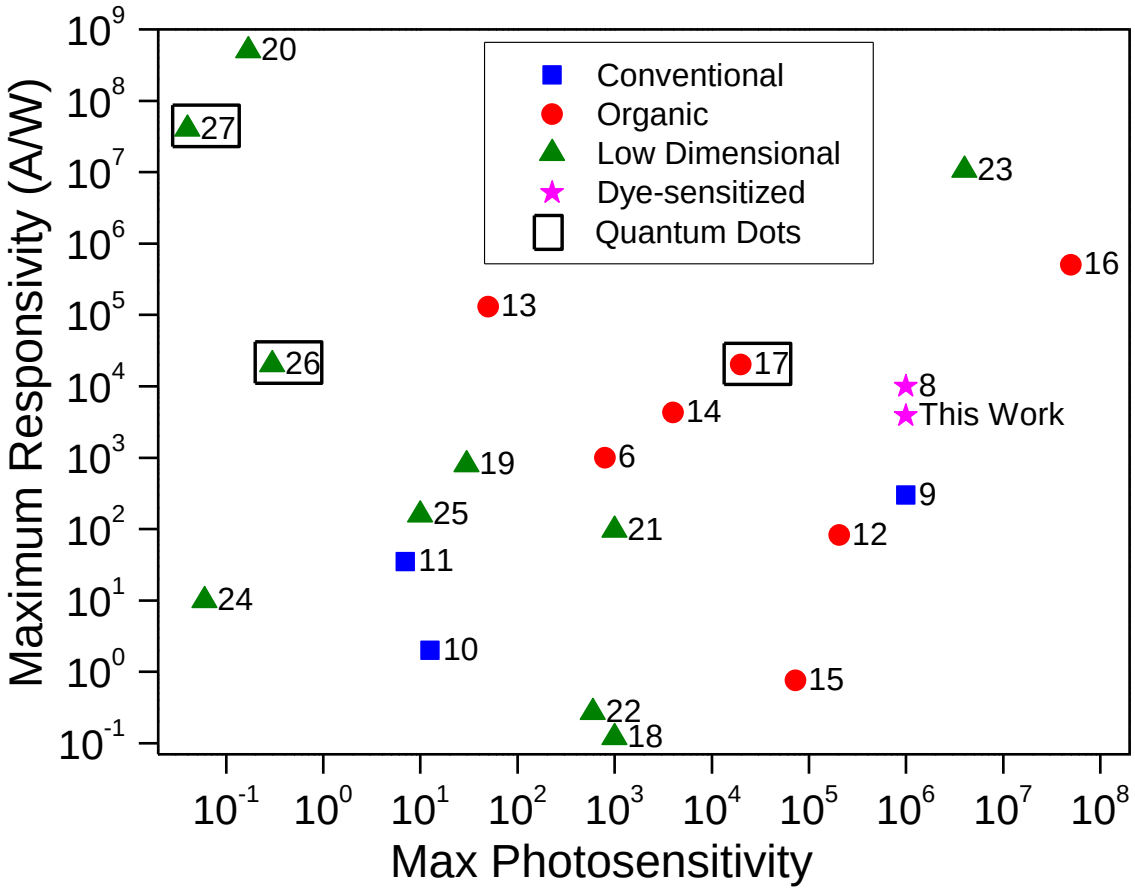

Figure 1. Maximum photosensitivity and responsivity values reported to date for various transistor-based photodetectors. For some device technologies the highest possible value of photosensitivity or responsivity had to be calculated indirectly from available data in the literature. The numbers next to the data indicate the reference from which the values were taken from.

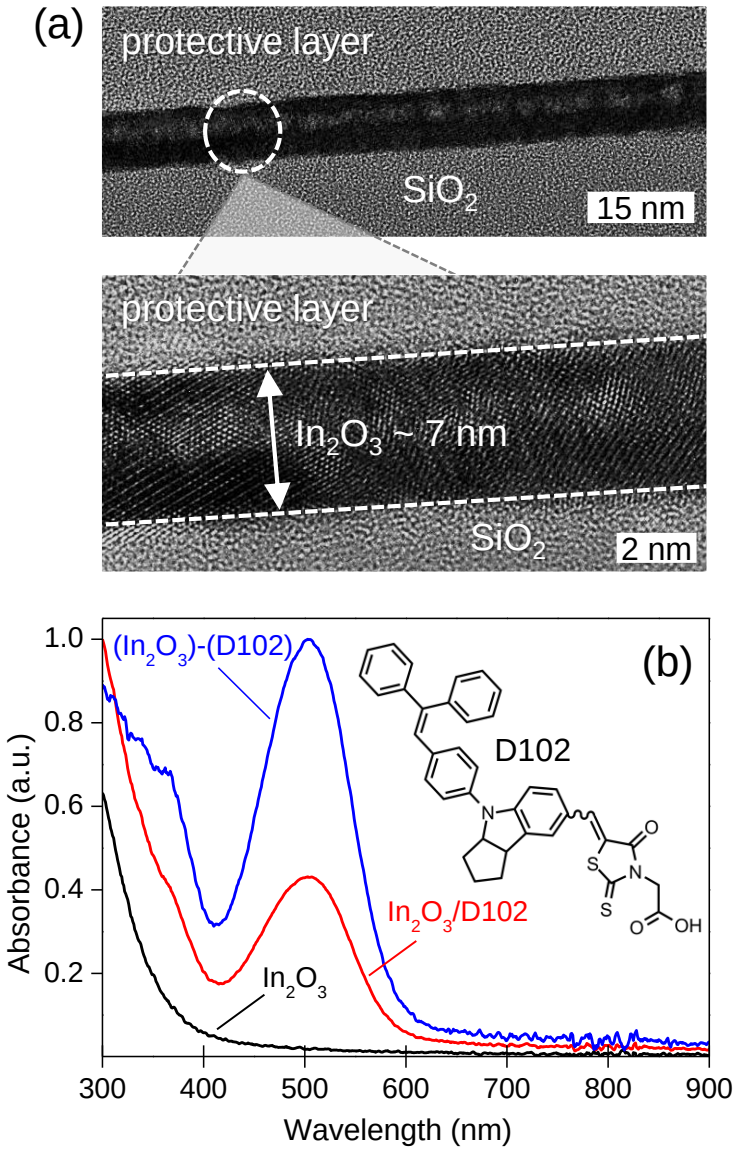

Figure 2. (a) Cross-sectional TEM images of an ultra-thin In_2O_3 layer grown by spin-coating on SiO_2. (b) Absorbance spectra of the pristine In_2O_3, the dye-functionalized In_2O_3/D102 bilayer and the difference due to D102 obtained by subtracting the absorbance of the In_2O_3 layer from that of the composite In_2O_3/D102 bilayer. Inset shows the molecular structure of the organic D102 dye.

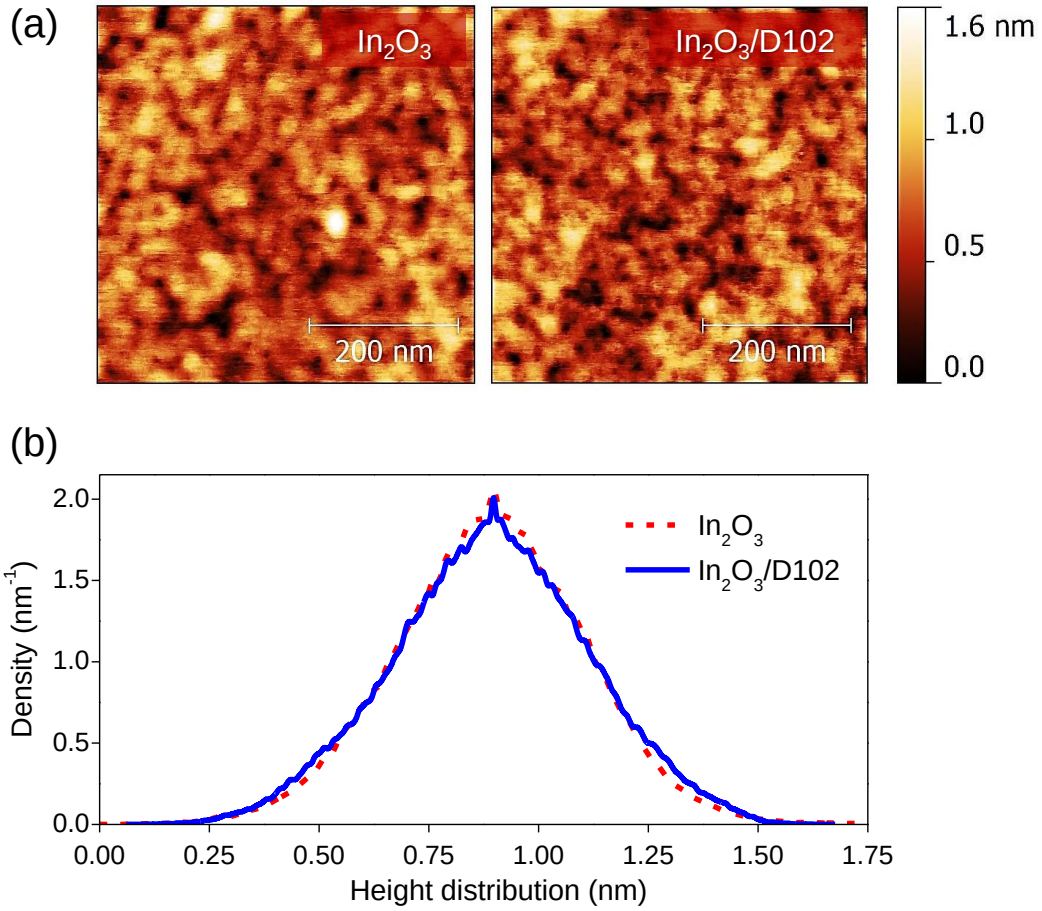

Figure 3. (a) AFM topography images of the pristine In_2O_3 and the D102-functionalized In_2O_3 layer, respectively. The RMS surface roughness values calculated from these images were very similar and on the order of 0.2 nm. (b) AFM height distributions for In_2O_3 and In_2O_3/D102 layers.

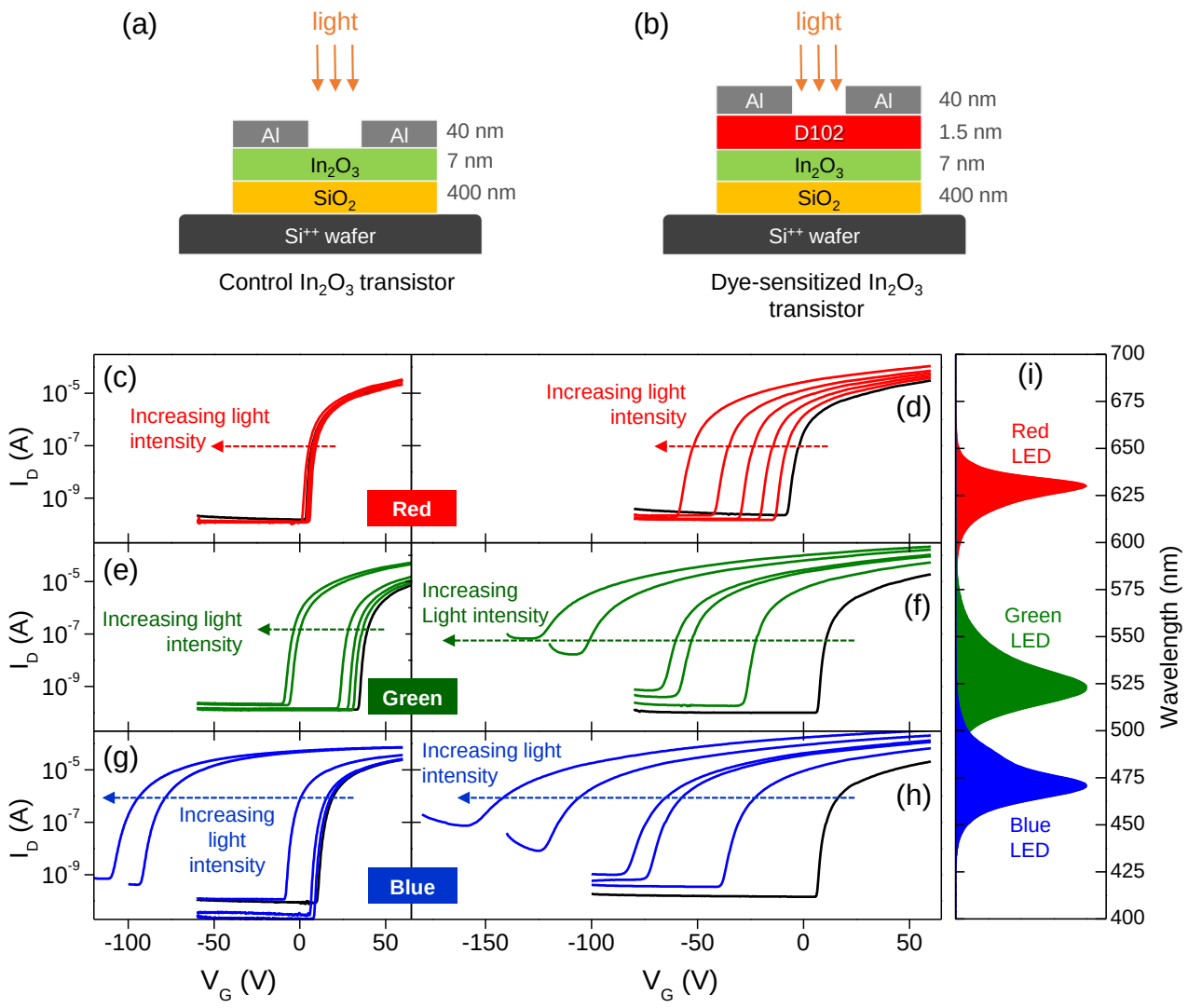

Figure 4. Structure of the control (a), and D102-sensitized In_2O_3 phototransistors (b) developed in this study. Panels (c), (e), and (g) show sets of the transfer characteristics measured for the control device under red, green and blue light illumination at different intensities. Panels (d), (f), and (h) display the transfer characteristics measured for the D102-sensitized In_2O_3 phototransistors under red, green and blue light illumination at different intensities. In each panel, black curves represent the transfer characteristics of the devices measured in the dark at $V_D = 5$ V. (i) Emission spectra of the three colors LEDs used in this study.

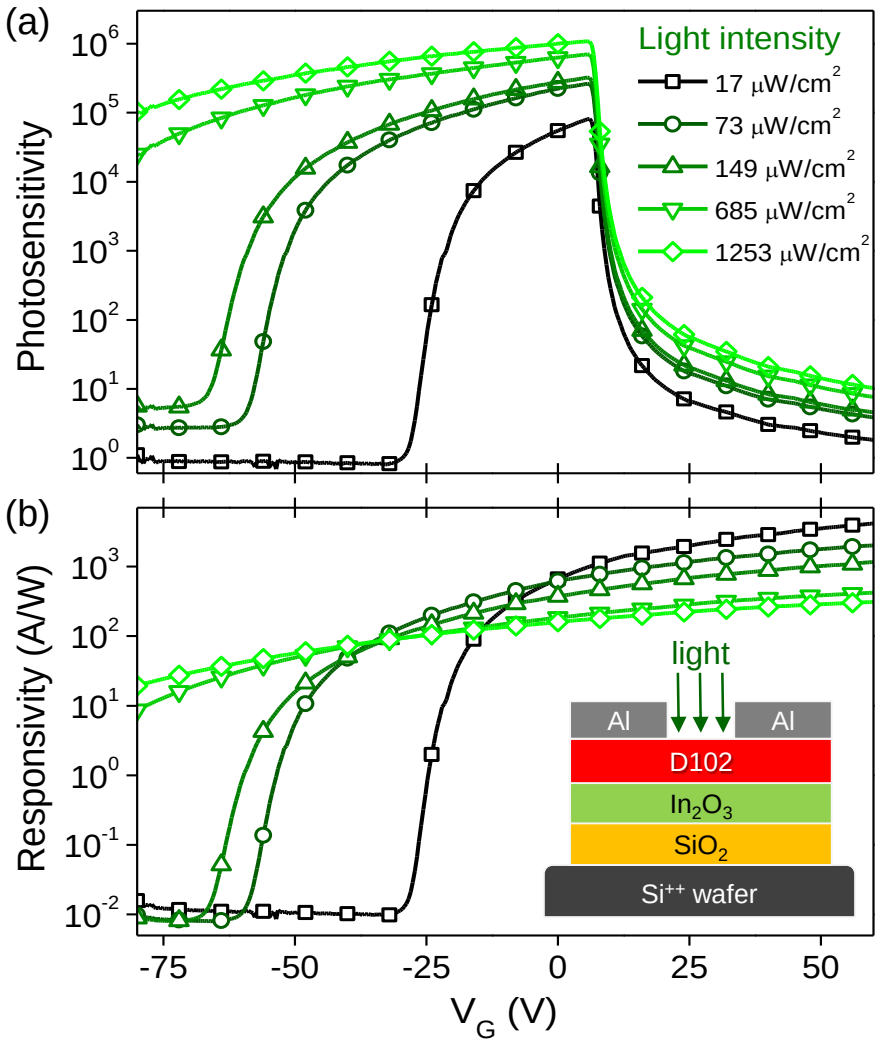

Figure 5. (a) Photosensitivity and (b) responsivity of the D102-sensitized In_2O_3 transistors measured at different green light illumination intensities and as a function of V_G at V_D = 5 V.. The inset in (b) shows the schematic of the D102-sensitized In_2O_3 phototransistor architecture employed.

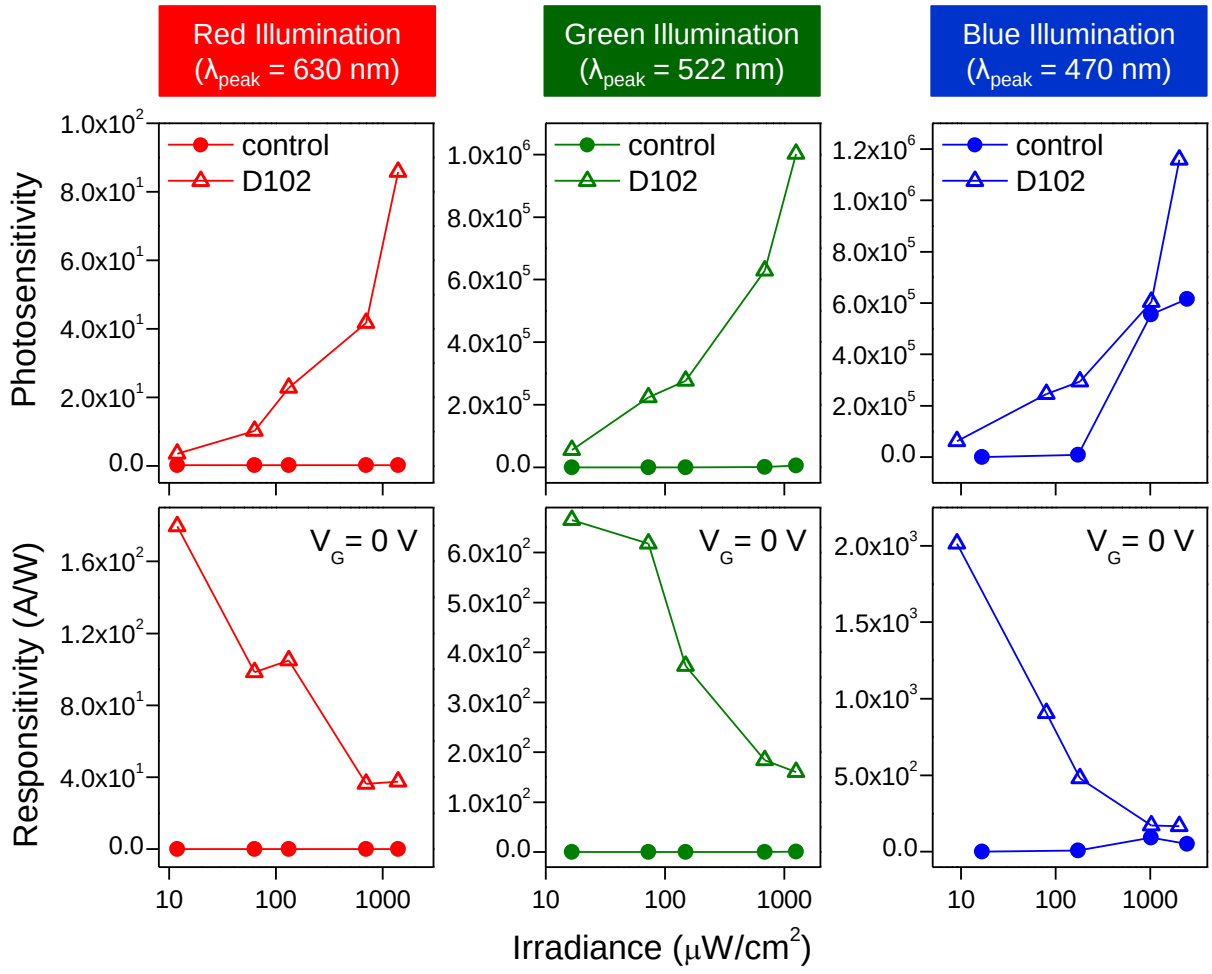

Figure 6. Photosensitivity and responsivity of control and D102-sensitized In_2O_3 phototransistors to red, green and blue light illumination at different intensities. Data were extracted from the transfer characteristics measured at $V_D = 5$ V.

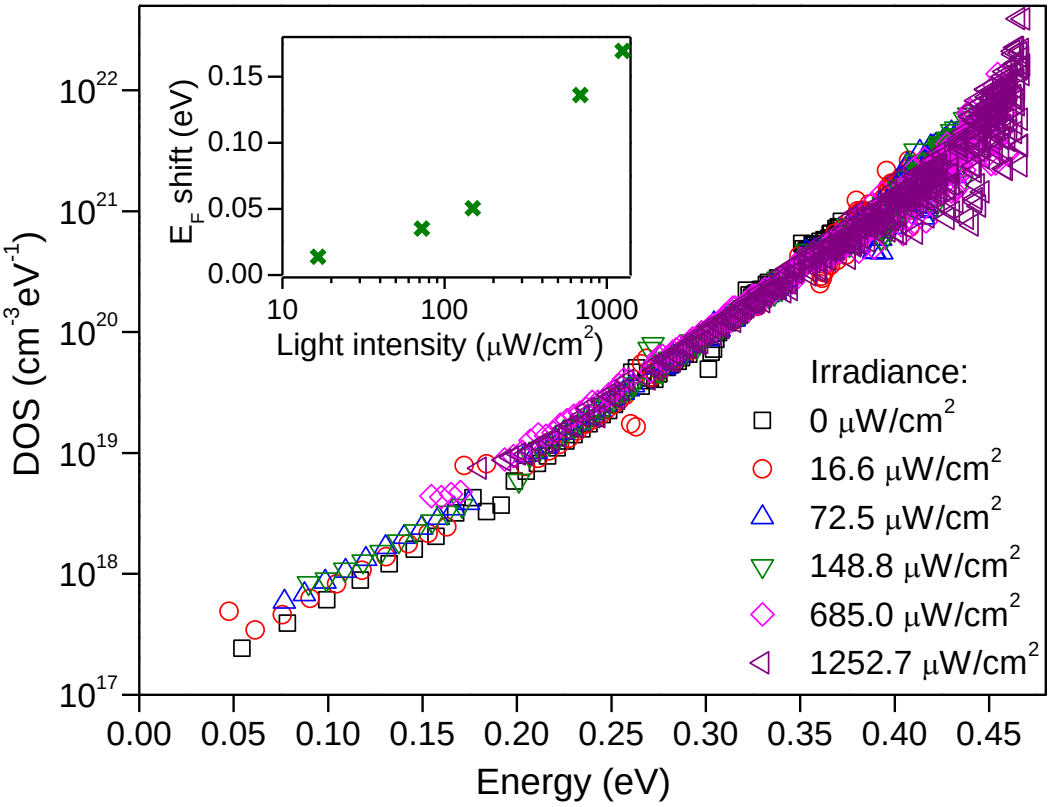

Figure 7. The aligned bandgap DOS of the D102 dye-sensitized device under multiple green illumination intensities. The origin of the energy axis is equal to the Fermi level in the semiconductor in the dark. The inset shows the shift in the Fermi level caused by green illumination-induced photodoping.

ASSOCIATED CONTENT

AUTHOR INFORMATION

Corresponding Authors

Prof. T. D. Anthopoulos

Department of Physics and Centre for Plastic Electronics

Blackett Laboratory, Imperial College London

London SW7 2AZ (United Kingdom)

E-mail: t.anthopoulos@ic.ac.uk;

Author Contributions

A.D.M, Y.-H.L, P.P., and T.D.A. designed the experiments and performed the AFM, TFT, UV-Vis measurements and wrote the relevant parts of the manuscript. K.Z. & A.A. performed the TEM measurements. All authors have given approval to the final version of the manuscript.

Funding Sources

A. M. and T.D.A. acknowledge the Engineering and Physical Sciences Research Council (EPSRC) grant number grant no. EP/G037515/1. P.P. acknowledges the Anandamahidol Foundation, Thailand, for financial support.

ACKNOWLEDGMENT

ABBREVIATIONS

Thin Film Transistor (TFT), Density of States (DOS), Transmission Electron Microscopy (TEM), Dye-Sensitized Solar Cell (DSSC), Light Emitting Diode (LED), Atomic Force Microscopy (AFM), Ultra-violet (UV), High Resolution Transmission Electron Microscopy (HR-TEM).

REFERENCES

(1) You, B. H.; Lee, B. J.; Lee, J. H.; Koh, J. H.; Kim, D.-K.; Takahashi, S.; Kim, N. D.; Berkeley, B. H.; Kim, S. S. 32.1: Invited Paper: LCD Embedded Hybrid Touch Screen Panel Based on a-Si:H TFT. *Dig. Tech. Pap. - Soc. Inf. Disp. Int. Symp.* **2009**, *40* (1), 439–442.

(2) Gidon, P.; Giffard, B.; Moussy, N.; Parrein, P.; Poupinet, L. Three Hydrogenated Amorphous Silicon Photodiodes Stacked for an above Integrated Circuit Colour Sensor. *Phys. status solidi* **2010**, *207* (3), 704–707.

(3) Jeon, S.; Ahn, S.-E.; Song, I.; Kim, C. J.; Chung, U.-I.; Lee, E.; Yoo, I.; Nathan, A.; Lee, S.; Robertson, J.; Kim, K. Gated Three-Terminal Device Architecture to Eliminate Persistent Photoconductivity in Oxide Semiconductor Photosensor Arrays. *Nat. Mater.* **2012**, *11* (4), 301–305.

(4) Weimer, P. K. The TFT - A New Thin-Film Transistor. *Proc. IRE* **1962**, *50* (6), 1462–1469.

(5) O'Regan, B.; Gratzel, M. A Low-Cost, High-Efficiency Solar Cell Based on Dye-Sensitized Colloidal TiO2 Films. *Nature* **1991**, *353*, 737–740.

(6) Guo, Y.; Du, C.; Di, C.; Zheng, J.; Sun, X.; Wen, Y.; Zhang, L.; Wu, W.; Yu, G.; Liu, Y. Field Dependent and High Light Sensitive Organic Phototransistors Based on Linear Asymmetric Organic Semiconductor. *Appl. Phys. Lett.* **2009**, *94* (14), 143303.

(7) Wu, H.-C.; Huang, Y.-C.; Ding, I.-K.; Chen, C.-C.; Yang, Y.-H.; Tsai, C.-C.; Chen, C.-D.; Chen, Y.-T. Photoinduced Electron Transfer in Dye-Sensitized SnO2 Nanowire Field-Effect Transistors. *Adv. Funct. Mater.* **2011**, *21* (3), 474–479.

(8) Pattanasattayavong, P.; Rossbauer, S.; Thomas, S.; Labram, J. G.; Snaith, H. J.; Anthopoulos, T. D. Solution-Processed Dye-Sensitized ZnO Phototransistors with Extremely High Photoresponsivity. *J. Appl. Phys.* **2012**, *112* (7), 074507–1 – 6.

(9) Johnson, N. M.; Chiang, a. Highly Photosensitive Transistors in Single-Crystal Silicon Thin Films on Fused Silica. *Appl. Phys. Lett.* **1984**, *45* (10), 1102.

(10) Ang, K.; Yu, M.; Lo, G.; Kwong, D. Low-Voltage and High-Responsivity Germanium Bipolar Phototransistor for Optical Detections in the Near-Infrared Regime. *IEEE Electron Device Lett.* **2008**, *29* (10), 1124–1127.

(11) Abid, K.; Khokhar, A. Z.; Rahman, F. High Responsivity Silicon MOS Phototransistors. *Sensors Actuators A Phys.* **2011**, *172* (2), 434–439.

(12) Noh, Y.-Y.; Kim, D.-Y.; Yoshida, Y.; Yase, K.; Jung, B.-J.; Lim, E.; Shim, H.-K. High-Photosensitivity P-Channel Organic Phototransistors Based on a Biphenyl End-Capped Fused Bithiophene Oligomer. *Appl. Phys. Lett.* **2005**, *86* (4), 043501.

(13) Noh, Y.-Y.; Kim, D.-Y.; Yase, K. Highly Sensitive Thin-Film Organic Phototransistors: Effect of Wavelength of Light Source on Device Performance. *J. Appl. Phys.* **2005**, *98* (7),

074505.

(14) Cho, M. Y.; Kim, S. J.; Han, Y. D.; Park, D. H.; Kim, K. H.; Choi, D. H.; Joo, J. Highly Sensitive, Photocontrolled, Organic Thin-Film Transistors Using Soluble Star-Shaped Conjugated Molecules. *Adv. Funct. Mater.* **2008**, *18* (19), 2905–2912.

(15) Liu, X.; Dong, G.; Duan, L.; Wang, L.; Qiu, Y. High Performance Low-Voltage Organic Phototransistors: Interface Modification and the Tuning of Electrical, Photosensitive and Memory Properties. *J. Mater. Chem.* **2012**, *22* (23), 11836.

(16) Xu, H.; Li, J.; Leung, B. H. K.; Poon, C. C. Y.; Ong, B. S.; Zhang, Y.; Zhao, N. A High-Sensitivity near-Infrared Phototransistor Based on an Organic Bulk Heterojunction. *Nanoscale* **2013**, *5* (23), 11850–11855.

(17) Sun, Z.; Li, J.; Yan, F. Highly Sensitive Organic near-Infrared Phototransistors Based on poly(3-Hexylthiophene) and PbS Quantum Dots. *J. Mater. Chem.* **2012**, *22* (40), 21673–21678.

(18) Choi, W.; Cho, M. Y.; Konar, A.; Lee, J. H.; Cha, G.-B.; Hong, S. C.; Kim, S.; Kim, J.; Jena, D.; Joo, J.; Kim, S. High-Detectivity Multilayer MoS(2) Phototransistors with Spectral Response from Ultraviolet to Infrared. *Adv. Mater.* **2012**, *24* (43), 5832–5836.

(19) Lopez-Sanchez, O.; Lembke, D.; Kayci, M.; Radenovic, A.; Kis, A. Ultrasensitive Photodetectors Based on Monolayer MoS2. *Nat. Nanotechnol.* **2013**, *8* (7), 497–501.

(20) Roy, K.; Padmanabhan, M.; Goswami, S.; Sai, T. P.; Ramalingam, G.; Raghavan, S.; Ghosh, A. Graphene-MoS2 Hybrid Structures for Multifunctional Photoresponsive Memory Devices. *Nat. Nanotechnol.* **2013**, *8* (11), 826–830.

(21) Abderrahmane, A.; Ko, P. J.; Thu, T. V; Ishizawa, S.; Takamura, T.; Sandhu, A. High Photosensitivity Few-Layered MoSe2 Back-Gated Field-Effect Phototransistors. *Nanotechnology* **2014**, *25* (36), 365202.

(22) Hwan Lee, S.; Lee, D.; Sik Hwang, W.; Hwang, E.; Jena, D.; Jong Yoo, W. High-Performance Photocurrent Generation from Two-Dimensional WS2 Field-Effect Transistors. *Appl. Phys. Lett.* **2014**, *104* (19), 193113.

(23) Jin, W.; Gao, Z.; Zhou, Y.; Yu, B.; Zhang, H.; Peng, H.; Liu, Z.; Dai, L. Novel Graphene–oxide–semiconductor Nanowire Phototransistors. *J. Mater. Chem. C* **2014**, *2* (9), 1592.

(24) Xu, H.; Wu, J.; Feng, Q.; Mao, N.; Wang, C.; Zhang, J. High Responsivity and Gate Tunable Graphene-MoS2 Hybrid Phototransistor. *Small* **2014**, *10* (11), 2300–2306.

(25) Tamalampudi, S. R.; Lu, Y.; Kumar U, R.; Sankar, R.; Liao, C.-D.; Moorthy B, K.; Cheng, C.; Chou, F. C.; Chen, Y. High Performance and Bendable Few-Layered InSe Photodetectors with Broad Spectral Response. *Nano Lett.* **2014**, *14* (5), 2800–2806.

(26) Sun, Z.; Liu, Z.; Li, J.; Tai, G.-A.; Lau, S.-P.; Yan, F. Infrared Photodetectors Based on CVD-Grown Graphene and PbS Quantum Dots with Ultrahigh Responsivity. *Adv. Mater.* **2012**, *24* (43), 1–6.

(27) Cheng, S.-H.; Weng, T.-M.; Lu, M.-L.; Tan, W.-C.; Chen, J.-Y.; Chen, Y.-F. All Carbon-Based Photodetectors: An Eminent Integration of Graphite Quantum Dots and Two Dimensional Graphene. *Sci. Rep.* **2013**, *3*, 2694.

(28) Yang, C.-Y.; Hwu, J.-G. Photo-Sensitivity Enhancement of HfO2-Based MOS Photodiode With Specific Perimeter Dependency Due to Edge Fringing Field Effect. *IEEE Sens. J.* **2012**, *12* (6), 2313–2319.

(29) Seo, S.-H.; Kim, K.-D.; Seo, M.-W.; Kong, J.-S.; Shin, J.-K.; Choi, P. Optical Characteristics of an N-Well / Gate-Tied PMOSFET-Type Photodetector with Built-in Transfer Gate for CMOS Image Sensor. *Sens. Mater.* **2007**, *19* (7), 435–444.

(30) Grünewald, M.; Thomas, P.; Würtz, D. A Simple Scheme for Evaluating Field Effect Data. *Phys. status solidi* **1980**, *100* (2), K139–K143.

(31) Kalb, W. L.; Batlogg, B. Calculating the Trap Density of States in Organic Field-Effect Transistors from Experiment: A Comparison of Different Methods. *Phys. Rev. B* **2010**, *81* (3), 035327.

(32) Spear, W. E. Drift Mobility Techniques for the Study of Electrical Transport Properties in Insulating Solids. *J. Non-Crystalline Solids 1* **1969**, *1* (3), 197–214.

(33) Le Comber, P. G.; Spear, W. E. Electronic Transport in Amorphous Silicon Films. *Phys. Rev. Lett.* **1970**, *25* (8), 509–511.

(34) Skinner, S. M. Diffusion, Static Charges, and the Conduction of Electricity in Nonmetallic Solids by a Single Charge Carrier. I. Electric Charges in Plastics and Insulating Materials. *J. Appl. Phys.* **1955**, *26* (5), 498–508.

(35) Lin, Y.-H.; Faber, H.; Labram, J. G.; Stratakis, E.; Sygellou, L.; Kymakis, E.; Hastas, N. a.; Li, R.; Zhao, K.; Amassian, A.; Treat, N. D.; McLachlan, M.; Anthopoulos, T. D. High Electron Mobility Thin-Film Transistors Based on Solution-Processed Semiconducting Metal Oxide Heterojunctions and Quasi-Superlattices. *Adv. Sci.* **2015**, *2, 1500058*.

(36) Labram, J. G.; Lin, Y.-H.; Zhao, K.; Li, R.; Thomas, S. R.; Semple, J.; Androulidaki, M.; Sygellou, L.; McLachlan, M.; Stratakis, E.; Amassian, A.; Anthopoulos, T. D. Signatures of Quantized Energy States in Solution-Processed Ultrathin Layers of Metal-Oxide Semiconductors and Their Devices. *Adv. Funct. Mater.* **2015**, *25* (11), 1727–1736.

(37) Labram, J. G.; Treat, N. D.; Lin, Y.-H.; Burgess, C. H.; McLachlan, M. A.; Anthopoulos, T. D. Energy Quantization in Solution-Processed Layers of Indium Oxide and Their Application in Resonant Tunneling Diodes. Adv. Funct. Mater. 2016, in press, DOI: 10.1002/adfm.201503732.

(38) Labram, J. G.; Lin, Y.-H.; Anthopoulos, T. D. Exploring Two-Dimensional Transport Phenomena in Metal Oxide Heterointerfaces for Next-Generation, High-Performance, Thin-Film Transistor Technologies. *Small* **2015**, *11* (41), 5472–5482.

(39) Park, H.; Bae, E.; Lee, J.-J.; Park, J.; Choi, W. Effect of the Anchoring Group in Ru−Bipyridyl Sensitizers on the Photoelectrochemical Behavior of Dye-Sensitized TiO 2

Electrodes: Carboxylate versus Phosphonate Linkages. *J. Phys. Chem. B* **2006**, *110* (17), 8740–8749.

(40) Nazeeruddin, M. K.; Humphry-Baker, R.; Liska, P.; Grätzel, M. Investigation of Sensitizer Adsorption and the Influence of Protons on Current and Voltage of a Dye-Sensitized Nanocrystalline TiO 2 Solar Cell. *J. Phys. Chem. B* **2003**, *107* (34), 8981–8987.

(41) Zhu, R.; Jiang, C.-Y.; Liu, B.; Ramakrishna, S. Highly Efficient Nanoporous TiO 2 - Polythiophene Hybrid Solar Cells Based on Interfacial Modification Using a Metal-Free Organic Dye. *Adv. Mater.* **2009**, *21* (9), 994–1000.

(42) Park, S. Y.; Kim, B. J.; Kim, K.; Kang, M. S.; Lim, K.-H.; Lee, T. Il; Myoung, J. M.; Baik, H. K.; Cho, J. H.; Kim, Y. S. Low-Temperature, Solution-Processed and Alkali Metal Doped ZnO for High-Performance Thin-Film Transistors. *Adv. Mater.* **2012**, *24* (6), 834–838.

(43) Jeong, J. K.; Won Yang, H.; Jeong, J. H.; Mo, Y.-G.; Kim, H. D. Origin of Threshold Voltage Instability in Indium-Gallium-Zinc Oxide Thin Film Transistors. *Appl. Phys. Lett.* **2008**, *93* (12), 123508.

(44) F ñrrn, P.; Riedl, T.; Kowalsky, W. Encapsulation of Zinc Tin Oxide Based Thin Film Transistors. *J. Phys. Chem. C* **2009**, *113* (25), 11126–11130.

(45) Moustakas, T. D.; Paul, W. Transport and Recombination in Sputtered Hydrogenated Amorphous Germanium. *Phys. Rev. B* **1977**, *16* (4), 1564–1576.

(46) Shur, M.; Hack, M.; Shaw, J. G. A New Analytic Model for Amorphous Silicon Thin Film Transistors. *J. Appl. Phys.* **1989**, *66* (7), 3371–3380.

(47) Fung, T.-C.; Chuang, C.-S.; Chen, C.; Abe, K.; Cottle, R.; Townsend, M.; Kumomi, H.; Kanicki, J. Two-Dimensional Numerical Simulation of Radio Frequency Sputter Amorphous In–Ga–Zn–O Thin-Film Transistors. *J. Appl. Phys.* **2009**, *106* (8), 084511.

(48) Caranzi, L.; Pace, G.; Guarnera, S.; Canesi, E. V; Brambilla, L.; Raavi, S. S. K.; Petrozza, A.; Caironi, M. Photoactive Molecular Junctions Based on Self-Assembled Monolayers of Indoline Dyes. *ACS Appl. Mater. Interfaces* **2014**, *6* (22), 19774–19782.

(49) Le Bahers, T.; Pauporté, T.; Scalmani, G.; Adamo, C.; Ciofini, I. A TD-DFT Investigation of Ground and Excited State Properties in Indoline Dyes Used for Dye-Sensitized Solar Cells. *Phys. Chem. Chem. Phys.* **2009**, *11* (47), 11276.

(50) Verbakel, F.; Meskers, S. C. J.; Janssen, R. a. J. Electronic Memory Effects in Diodes of Zinc Oxide Nanoparticles in a Matrix of Polystyrene or poly(3-Hexylthiophene). *J. Appl. Phys.* **2007**, *102* (8), 083701.

(51) Lakhwani, G.; Roijmans, R. F. H.; Kronemeijer, A. J.; Gilot, J.; Janssen, R. a. J.; Meskers, S. C. J. Probing Charge Carrier Density in a Layer of Photodoped ZnO Nanoparticles by Spectroscopic Ellipsometry. *J. Phys. Chem. C* **2010**, *114* (35), 14804–14810.

(52) Kim, K. T.; Lee, K.; Oh, M. S.; Park, C. H.; Im, S. Surface-Induced Time-Dependent

Instability of ZnO Based Thin-Film Transistors. *Thin Solid Films* **2009**, *517* (23), 6345–6348.

(53) Shockley, W. *Electrons and Holes in Semiconductors with Applications to Transistor Electronics*; D. Van Nostrand Company Inc., 1959; Vol. 5.

(54) Lee, K.; Oh, M. S.; Mun, S.; Lee, K. H.; Ha, T. W.; Kim, J. H.; Park, S.-H. K.; Hwang, C.-S.; Lee, B. H.; Sung, M. M.; Im, S. Interfacial Trap Density-of-States in Pentacene- and ZnO-Based Thin-Film Transistors Measured via Novel Photo-Excited Charge-Collection Spectroscopy. *Adv. Mater.* **2010**, *22* (30), 3260–3265.

(55) Bubel, S.; Mechau, N.; Hahn, H.; Schmechel, R. Trap States and Space Charge Limited Current in Dispersion Processed Zinc Oxide Thin Films. *J. Appl. Phys.* **2010**, *108* (12), 124502.

(56) Nyft¨q+T-: @khunu+X- H: Klt+B-: Sdj d+ `-: Qdrgbghj nu+L - `-: Cnf˜m+R-: @uqt shm+U-: Bgn+R–I-: L nqj nb, H. A Comprehensive Review of ZnO Materials and Devices. *J. Appl. Phys.* **2005**, *98* (4), 041301.

(57) Aljishi, S.; Cohen, J. D.; Jin, S.; Ley, L. Band Tails in Hydrogenated Amorphous Silicon and Silicon-Germanium Alloys. *Phys. Rev. Lett.* **1990**, *64* (23), 2811–2814.

(58) Cody, G. D.; Tiedje, T.; Abeles, B.; Brooks, B.; Goldstein, Y. Disorder and the Optical-Absorption Edge of Hydrogenated Amorphous Silicon. *Phys. Rev. Lett.* **1981**, *47* (20), 1480–1483.

(59) Pattanasattayavong, P. Solution-Processable Hole-Transporting Inorganic Semiconductors for Electronic Applications, Ph.D. Dissertation, Imperial College London, 2015.

(60) Kalb, W.; Meier, F.; Mattenberger, K.; Batlogg, B. Defect Healing at Room Temperature in Pentacene Thin Films and Improved Transistor Performance. *Phys. Rev. B* **2007**, *76* (18), 184112.

Table of Contents Graphic

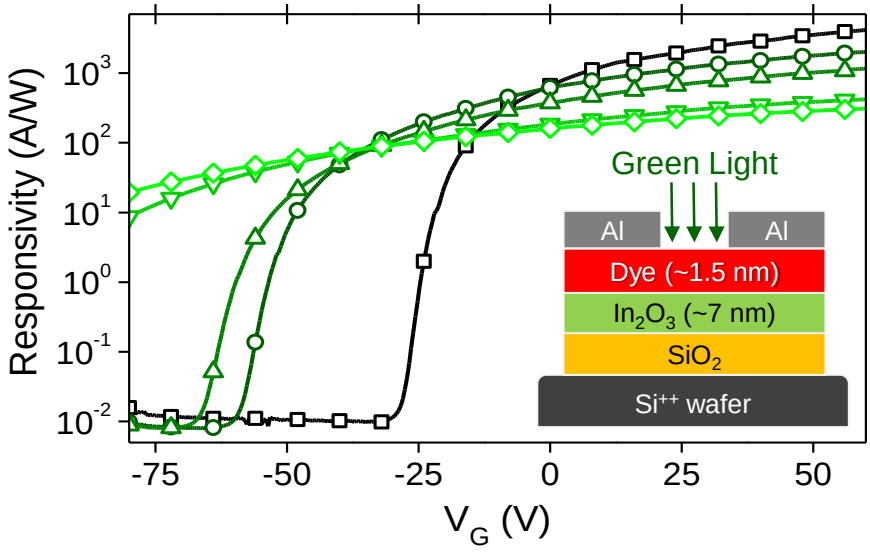

Synopsis

Solution-processed dye-sensitized phototransistors consisting of an ultra-thin layer of indium oxide the surface of which is functionalized with the light-absorbing dye D102 are demonstrated. The phototransistors preferential color photoresponse centered at ~500 nm with maximum photosensitivity and responsivity values of ~10^6 and ~2×10^3 A/W, respectively (Image).